The IEEE Reliability Test System: A Proposed 2019 Update

Clayton Barrows , *Member, IEEE*, Aaron Bloom, *Member, IEEE*, Ali Ehlen , Jussi Ikäheimo ,
Jennie Jorgenson , *Member, IEEE*, Dheepak Krishnamurthy , *Member, IEEE*, Jessica Lau , *Member, IEEE*,
Brendan McBennett, Matthew O'Connell , *Member, IEEE*, Eugene Preston , *Life Senior Member, IEEE*,
Andrea Staid , Gord Stephen , *Member, IEEE*, and Jean-Paul Watson , *Member, IEEE*

Abstract—The evolving nature of electricity production, transmission, and consumption necessitates an update to the IEEE's Reliability Test System (RTS), which was last modernized in 1996. The update presented here introduces a generation mix more representative of modern power systems, with the removal of several nuclear and oil-generating units and the addition of natural gas, wind, solar photovoltaics, concentrating solar power, and energy storage. The update includes assigning the test system a geographic location in the southwestern United States to enable the integration of spatio-temporally consistent wind, solar, and load data with forecasts. Additional updates include common RTS transmission modifications in published literature, definitions for reserve product requirements, and market simulation descriptions to enable benchmarking of multi-period power system scheduling problems. The final section presents example results from a production cost modeling simulation on the updated RTS system data.

Index Terms—Power system economics, power system planning, power system reliability, power system modeling, power system operations, reliability test system, production cost modeling, exact reliability indices, benchmarking.

I. INTRODUCTION

NEW questions are arising regarding power systems of the future as new sources of generation enter the market and traditional fuel sources retire at a rapid rate. These changes bring with them new challenges and opportunities to meet reliability and security requirements at minimum cost. The IEEE has maintained a collection of test systems for several decades to assist

C. Barrows, A. Bloom, A. Ehlen, J. Jorgenson, D. Krishnamurthy, J. Lau, B. McBennett, M. O'Connell, and G. Stephen are with the National Renewable Energy Laboratory, Lakewood, CO 80401 USA (e-mail: clayton.barrows@nrel.gov; aaron.bloom@nrel.gov; ali.ehlen@gmail.com; jennie.jorgenson@nrel.gov; dheepak.krishnamurthy@nrel.gov; jessica.lau@nrel.gov; brendan.mcbennett@colorado.edu; matthew.oconnell@nrel.gov; Gord.Stephen@nrel.gov).

J. Ikäheimo is with the VTT Technical Research Center of Finland, 02044 Espoo, Finland (e-mail: Jussi.Ikaheimo@vtt.fi).

E. Preston is with the Transmission Adequacy Consulting, Austin, TX 78735 USA (e-mail: g.preston@ieee.org).

A. Staid and J.-P. Watson are with the Sandia National Laboratories, Albuquerque, NM 87185 USA (e-mail: astaid@sandia.gov; jwatson@sandia.gov).

Color versions of one or more of the figures in this paper are available online at http://ieeexplore.ieee.org.

Digital Object Identifier 10.1109/TPWRS.2019.2925557

the engineering community in understanding how new technologies and operational practices might impact power system cost and performance. In this context we introduce a substantial update to the IEEE Reliability Test System (RTS). In keeping with the intent of prior work, we re-emphasize that the goal of the IEEE RTS family is *not* to reflect or represent a specific, real power system. Rather, these test systems should represent technologies and configurations that could be encountered in any system. In this most recent update to the RTS, we aim to continue the tradition of providing a model that allows researchers to explore a variety of current and future conditions that power system operators might face.

As part of the United States Department of Energy's Grid Modernization Initiative we developed several critical updates to the RTS. We modernize the sources of generation by adding natural gas, wind, solar photovoltaics (PV), concentrating solar power (CSP) and storage to the model. We also add geographic and temporal variability in the form of 5-minute load, wind and solar data; each with a corresponding hourly time series representing day-ahead forecasts based on weather patterns experienced in the Southwestern United States. By providing a modernized generation fleet, along with geographically and temporally consistent weather-driven time series data, we fill a gap in the existing suite of test systems published by IEEE and others and enable a variety of modeling and analysis explorations with a dataset that is large enough to demonstrate the complexity of power system operation and planning, yet small enough so that novel techniques can be applied and results can be understood [1]. We present results from a benchmark case and a suite of analyses conducted with the modernized test system. Finally, we detail our goals for online collaboration and continued test system evolution, via a publicly available GitHub repository, by enabling and encouraging other users to share their dataset modifications with the broader community.

II. HISTORY OF THE RELIABILITY TEST SYSTEM

The first version of the IEEE Reliability Test System (RTS-79) was developed and published in 1979 by the Application of Probability Methods (APM) Subcommittee of the Power System Engineering Committee [2]. RTS-79 was developed to satisfy the need for a standardized model to test and compare results

TABLE I
RTS-79 GENERATION MIX

Prime Mover	Fuel	Capacity-MW	(%)
Steam	Fossil-Oil	951	28
Steam	Fossil-Coal	1,274	37
Steam	Nuclear	800	24
Combustion Turbine	Fossil-Oil	80	2
Hydro	Hydro	300	9
–	**Total**	3,405	100

TABLE II
HEDMAN et al. BUS LOAD CHANGES

Bus	RTS-96 Load-MW	RTS-GMLC Load-MW
13	265	745
14	194	80
15	317	132
19	181	75
20	128	53

from different power system reliability evaluation methodologies. The model was specifically designed to conduct analyses of the impact of generation and transmission outages on the system. Table I describes the RTS-79 generation mix. A few noteworthy limitations of the RTS-79 include the lack of load uncertainty or load diversity across the buses. Additionally, the model relies on representative weeks for peak seasonal conditions.

The RTS-79 received a modest update in 1986 (RTS-86) [3]. In this update particular attention was paid to improving information relating to the generation fleet. Some key features added in this update include: unit derates (partial outages), load forecast uncertainty and unit scheduled maintenance. In addition to improvements related to reliability indices such as loss of load probability (LOLP), loss of load expectation (LOLE) and loss of energy expectation (LOEE), the model was doubled in size to enable users to explore multi-area interconnection effects. The RTS-86 joined two identical RTS-79 models with a single 230 kV tie line with a rating of 300 MW. For benchmarking purposes, the RTS-86 also presents exact system reliability indices.

The most recent update to the RTS came in 1996 (RTS-96) [4]. This update provided a substantial increase in model complexity and size; the RTS-96 consists of three joined RTS-79 models. At the time, industry was experiencing a dramatic increase in interregional transactions and improvements in computing power. Thus, larger multi-area models could be tractably analyzed. The most substantial addition to the RTS-96 was the inclusion of operating costs and constraints related to the generating units, specifically: unit start-up heat input, net plant incremental heat rates, unit cycling restrictions, ramping rates, and unit emissions data. This update also added new transmission technologies to the model: a phase shifter, a two terminal DC transmission line and five inter-area AC ties. Among the RTS-96, the 89-bus PEGASE case, and the IEEE 57, 118, and 300 bus test systems, which all present networks of similar size, only the RTS-96 specifies generator costs, generator technical parameters, and transmission flow limits, making the published RTS-96 dataset uniquely suitable for method development and analysis that considers the economics of power systems operations and planning [5], [6].

III. RTS-GMLC

The IEEE RTS is intended to serve as a platform for analyzing power system operations strategies and issues, including unit commitment (UC), economic dispatch (ED), load flow and associated economic and reliability impacts. To that end, the RTS should enable researchers to consider relationships between a variety of resources under a plausible set of system conditions. Additionally, the system should be sufficiently complex to approximate the scale of challenges that might be expected in a modern power system. The RTS generation mix has remained constant since 1979. In each subsequent release of the model, the original model was replicated, with the generation fleet and mix static.

Power systems in many parts of the world are changing rapidly with the proliferation of energy markets, environmental policies, and evolving technology and fuel costs. In the United States, natural gas combined cycle, wind, and solar generators are displacing coal and oil fueled generation. At the same time, the need to understand reliability is expanding. While power system engineers have typically looked at system response under contingency conditions, there is increased interest in understanding the flexibility challenges of modern power systems associated with UC and ED of an increasingly variable and uncertain generation fleet. To reflect the above changes to power systems composition, we implemented a variety of updates to the RTS, resulting in the RTS-Grid Modernization Laboratory Consortium (RTS-GMLC) model. The RTS-GMLC features several key changes from the RTS-96, which ultimately enable year-long simulations of hourly and 5-minute operations with a modern generation fleet.

The following subsections outline the process used to modify the RTS-96 model. First, we adopted changes documented in the literature to increase the occurrence of congestion in ED problems (Hedman et al. updates) [7]. Then, we updated the generation fleet to reflect some of the evolutionary trends recently witnessed in real-world power systems (GMLC updates).

A. Hedman et al. Updates

In its published form, the RTS-96 has no binding transmission constraints in the context of UC/ED analysis. To enhance the realism and complexity of UC/ED analysis of the RTS, Hedman et al. make a series of modifications that add transmission congestion based on changes proposed by McCalley et al. and Motto et al. [7]–[9]. Specifically, we removed the transmission lines connecting buses 11 and 13 in each region[1] and reduced the capacity of the lines connecting buses 14 and 16 in each region to 350 MW. We modified the load in each region at buses 13, 14, 15, 19, and 20 according to the data described in Table II.

---

[1]The RTS has three regions, distinguished by the hundreds digit in the node number. For example, when bus 13 is mentioned, it refers to nodes 113, 213 and 313.
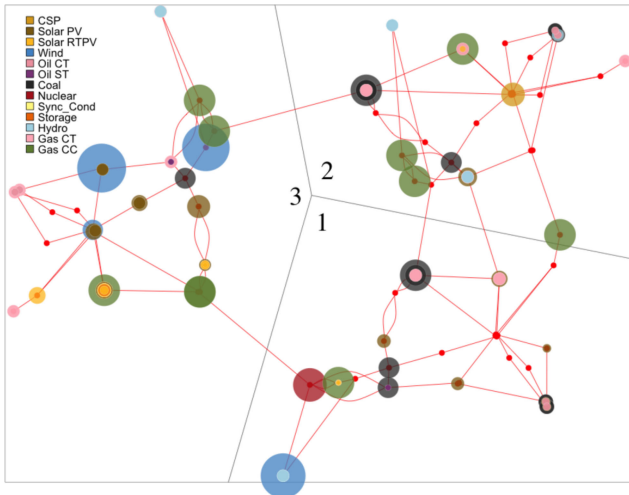
Fig. 1.   The network layout of the RTS-GMLC, annotated with the relative size and location of RTS-GMLC generation capacity.

Fig. 2.   Transmission, wind, and solar geospatial data layers used to add temporal and geographic diversity to the RTS-GMLC model.

B. GMLC Updates

Many of the challenges faced in modern power systems operations are driven by the proliferation of variable energy resources, namely wind and solar generators. These resources rely upon location and time dependent weather patterns for energy production. To represent wind and solar generators in the RTS, we generated relative node locations based upon the RTS-96 transmission line distances and then projected the network on an arbitrary geographic location in the southwestern United States. The RTS layout, shown in Fig. 1, covers a geographical region of roughly 250×250 miles and was projected onto an area extending roughly from Los Angeles to Las Vegas to obtain a reference for load, wind, solar, and hydrologic time series data population. This location was chosen because it included adequate available energy for each technology. While projecting the RTS model onto the southwestern United States enables the use of geospatially and temporally coincident weather-driven data, it would be inappropriate to use the projected RTS model to provide insights into the real-world power system in this location.

To reflect the diversity of electricity demand patterns, balancing authorities that operate in or near the geographic RTS projection were chosen to represent each of the three RTS regions. The balancing authority load profiles were drawn from the dataset used in the Western Wind and Solar Integration Study Phase 2 (WWSIS-2), which is based on the WECC TEPPC 2020 Common Case [10], [11]. The three load profiles were then normalized to the peak regional load in the RTS (2850 MW). The RTS-GMLC model provides two load time series for each region: a rolling 24-hour ahead forecast at hourly resolution and an "actual" load profile at 5-minute resolution. Nodal load time series data were derived from the static peak load distribution in the RTS power flow case.

Generation profiles for wind, utility PV, rooftop PV, and hydro were also selected from the WWSIS-2 dataset [10]. In order to match the geographic extent of the network, wind and PV resource geospatial data layers were combined with transmission
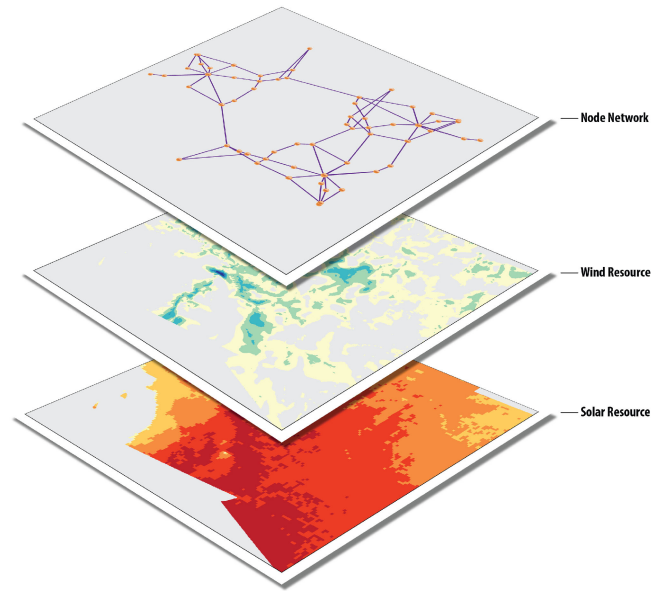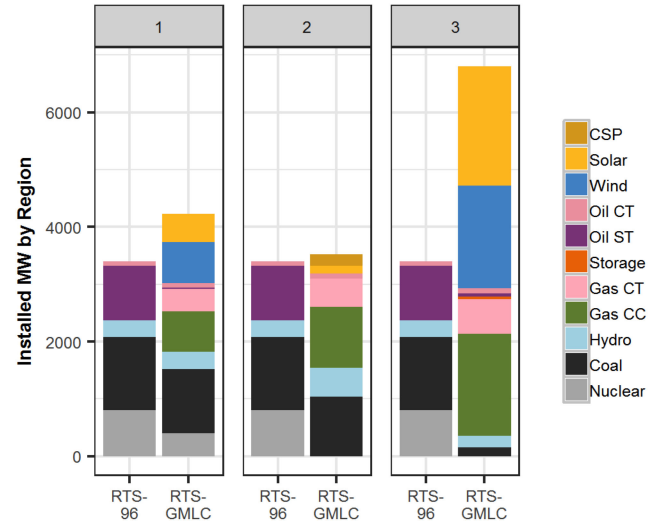

Fig. 3.   Changes in regional generation capacity mix between the RTS-96 and RTS-GMLC.

data as shown in Fig. 2. Since the WWSIS-2 dataset contains significantly more local capacity than is appropriate to include in the RTS, specific wind and PV generators were selected at random from the set of WWSIS-2 generators to achieve the regional capacity mix (see Fig. 3). Wind and utility-scale PV generators were connected to the nearest generation bus in the geo-located RTS. Rooftop PV generators were connected to the nearest load bus. PV profiles were generated using the System Advisor Model (SAM) with 2006 meteorology [12]. Wind data was derived from the WWSIS-2 dataset.[2] The RTS-GMLC model includes both hourly and 5-minute resolution wind and solar profiles.

[2]All generation profiles were adjusted in the WWSIS-2 project to be time synchronized to the year 2020.

The hourly profiles represent rolling 24-hour ahead forecasted energy production for each generator, while the 5-minute profiles represent each generator's "actual" energy production. The details of the forecasting method are described in [10].

CSP has generator characteristics that are driven by solar irradiance and a variety of more traditional steam generator operating constraints. CSP can be bundled with thermal energy storage (TES) to provide a variety of grid services including balancing and time shifting of demand. The RTS-GMLC adopts the representation of CSP-TES developed in [13] and detailed in [14]. The representation utilizes SAM to calculate solar availability and then dispatches the steam turbine portion of the plant given the constraints of solar energy and operating characteristics of the turbine itself. The modeled CSP-TES plant uses a solar field to power block ratio (solar multiple) of 1.6 and has six hours of thermal storage when operating at max capacity.

The economic competitiveness and technical capabilities of energy storage are evolving to impact how load is balanced in modern power systems. Energy storage can change demand patterns and provide a full suite of energy and ancillary services. The RTS-GMLC update incorporates the energy storage resource capabilities described in Denholm *et al.* [15]. The storage device included in the RTS-GMLC dataset is a battery storage device with a maximum charge and discharge rate of 50 MW, a round-trip efficiency of 85%, and a usable energy storage capacity of up to 150 MWh. In other words, the fully charged battery can operate at maximum discharge rate for a three hour duration, denoting an energy-to-power ratio of three. It solely performs energy arbitrage (i.e., does not provide reserves) and has unbounded ramp rates and no other operational constraints. However, its representation can be easily altered to allow users to model other forms of energy storage and allow it to provide additional services.

The fossil generating fleet of the RTS-96 and prior models was upgraded to reflect an evolving, modern generation mix. Some of the coal and oil fueled generation in the RTS-96 were replaced with 55 MW natural gas fired combustion turbines (GasCT) and 350 MW natural gas fired combined cycle (GasCC) generators. Generator operating and emissions data for the natural gas fired generators and missing data for other generators were adopted from generation type specific capacity weighted averages of the following WWSIS-2 generation fleet parameters: relative minimum generation levels, relative ramp rates, forced and planned outage rates, and repair and maintenance times [10]. Startup parameters (start time, start heat, and minimum up/down time) were based on turbine manufacturer data [16]–[19]. The changes to the overall generation mix for each region are shown in Fig. 3 and are summarized for conventional plants (excluding wind and solar) in Table III. In Table III, 'Group' corresponds to the naming system used in the RTS-96 [4] and 'Cap-MW' indicates the installed capacity of each unit.

To reflect the uniqueness and diversity of individual generation plants, we provide heat-rate parameters for each plant. Four point heat rate curves are derived from the Environmental Protection Agency Clean Air Markets database [20]. Individual heat rate curves are assigned to RTS generators by random selection from the U.S. plant population, filtered by plant type and size.

TABLE III
RTS-GMLC CONVENTIONAL GENERATING UNIT CHANGES

Region	BusID	Group	Cap-MW	Type	Units	Add/Rm
1	107	U100	80	Oil/ST	3	Remove
1	113	U197	95.1	Oil/ST	3	Remove
1	115	U12	12	Oil/ST	3	Remove
1	118	U400	400	Nuclear	1	Remove
1	123	U155	155	Coal/ST	1	Remove
2	201	U76	76	Coal/ST	1	Remove
2	207	U100	80	Oil/ST	3	Remove
2	213	U197	95.1	Oil/ST	3	Remove
2	215	U155	155	Coal/ST	1	Remove
2	215	U12	12	Oil/ST	5	Remove
2	221	U400	400	Nuclear	1	Remove
3	301	U76	76	Coal/ST	2	Remove
3	302	U76	76	Coal/ST	2	Remove
3	307	U100	80	Oil/ST	3	Remove
3	313	U197	95.1	Oil/ST	3	Remove
3	315	U155	155	Coal/ST	1	Remove
3	318	U400	400	Nuclear	1	Remove
3	321	U400	400	Nuclear	1	Remove
3	322	U50	50	Hydro	2	Remove
3	323	U155	155	Coal/ST	2	Remove
3	323	U350	350	Coal/ST	1	Remove
1	107	U350	35	GasCC	1	Add
1	113	U55	55	GasCT	4	Add
1	118	U350	350	GasCC	1	Add
1	123	U55	55	GasCT	3	Add
2	201	U50	50	Hydro	1	Add
2	207	U55	55	GasCT	2	Add
2	213	U55	55	GasCT	2	Add
2	213	U350	350	GasCC	1	Add
2	215	U50	50	Hydro	3	Add
2	215	U55	55	GasCT	2	Add
2	218	U350	350	GasCC	1	Add
2	221	U350	350	GasCC	1	Add
2	223	U55	55	GasCT	3	Add
3	301	U55	55	GasCT	2	Add
3	302	U55	55	GasCT	2	Add
3	307	U55	55	GasCT	2	Add
3	313	U350	350	GasCC	1	Add
3	315	U55	55	GasCT	3	Add
3	318	U350	350	GasCC	1	Add
3	321	U350	350	GasCC	1	Add
3	322	U55	55	GasCT	2	Add
3	323	U350	350	GasCC	2	Add

Fig. 4 shows the diversity of the RTS-GMLC heat-rates relative to the RTS-96 data. In addition to providing a generation fleet with unique and realistic heat rate and operating cost parameters, heat-rate diversity can help generate optimization problems with unique optimal solutions and help improve optimization solver performance by avoiding symmetry.

Finally, the RTS-GMLC includes three operational reserve product definitions, summarized in Table IV, for co-optimized energy and reserve scheduling. Flexibility and regulation reserves are defined in both upward and downward directions, while spinning reserves are only defined in the upward direction. Each reserve product is characterized by the timeframe in which any capacity satisfying the requirement must be able to respond. Reserve requirements are provided as time series for each reserve product. The spinning reserve requirements are defined as 3% of the regional load profiles. The flexibility and regulation reserves are calculated using the methodology described in Ibanez *et al.* [21].
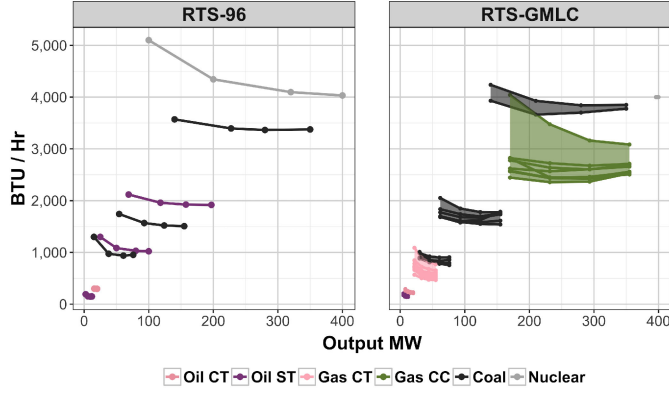
Fig. 4. Average hourly heat-rates by plant output levels for each unit type in the RTS-96 and RTS-GMLC. Shaded regions represent the range of individual heat-rate values for each unit group.

TABLE IV
RTS-GMLC RESERVE PRODUCTS

Reserve Product	Spin$_{Up}$	Flex$_{Up}$	Flex$_{Dn}$	Reg$_{Up}$	Reg$_{Dn}$
Timeframe (minutes)	10	20	20	5	5

C. Online Publication

The RTS-GMLC is publicly available online via GitHub: https://github.com/GridMod/RTS-GMLC [22].

IV. APPLICATION

A key application of the updated RTS model is in production cost modeling. Production cost models (PCMs) are a class of models used to simulate electric power system operations and have become increasingly important as system planners and operators face more decisions regarding how to manage large systems under increasing amounts of uncertainty. PCMs can inform planner, operator, and policy maker decisions by simulating detailed system operations under a variety of posited conditions. Modern PCMs simulate electricity markets by formulating variations of UC and ED for generator and load scheduling [23]. Many of the updates described in Section III are focused on improving the realism of PCM analyses conducted using RTS models. The details of a PCM and the associated UC, ED, and power flow formulations vary widely depending on the package and options. Therefore, the following subsection presents an example formulation that includes many of the features commonly represented in PCMs.

In addition to the PCM application, the RTS-GMLC dataset is compatible with several other traditional power system analysis tools and includes formatted files for use in PSS/E and MAT-POWER. PSS/E and MATPOWER allow for a suite of power system simulations including power flow, optimal power flow, transient stability, voltage stability, and contingency analysis [24], [25]. Furthermore, the RTS-GMLC dataset intentionally includes more generation capacity than is required to simulate reliable power system operations. The overbuilt nature of the

RTS-GMLC allows users to explore the impacts of different generation and transmission configurations.

A. Example PCM Formulation

$$\text{min.} \quad \sum_t \sum_k c_k^t g_k^t + c_k^{t,su} su_k^t + c_k^{t,sd} sd_k^t \quad (1)$$

s.t.

$$\sum_k g_k^t = \sum_i l_i^t \quad \forall \ t \quad (2)$$

$$G_k^{t,MIN} u_k^t \le g_k^t \le G_k^{t,MAX} u_k^t \quad \forall \ t,k \quad (3)$$

$$M_k^{t,down} \le g_k^t - g_k^{t-1} \le M_k^{t,up} \quad \forall \ t,k \quad (4)$$

$$u_k^{t-1} - u_k^t + su_k^t - sd_k^t = 0 \quad \forall \ t,k \quad (5)$$

$$\sum_{t \in h} g_k^t \le E_k^{h,MAX} \quad \forall \ k,h \quad (6)$$

$$\sum_j f_{i,j}^t = \sum_k (g_{k \in i}^t) - l_i^t \quad \forall \ t,i \quad (7)$$

$$f_{i,j}^t = B_{i,j}(\theta_i^t - \theta_j^t) \quad \forall \ t,i,j \quad (8)$$

$$\theta^{MIN} \le \theta_i^t \le \theta^{MAX} \quad \forall \ t,i \quad (9)$$

$$f_{i,j}^{t,MIN} \le f_{i,j}^t \le f_{i,j}^{t,MAX} \quad \forall \ t,i,j \quad (10)$$

$$u, su, sd \ \in \ \{0,1\} \quad (11)$$

Equations (1)–(11) provide a simplified example PCM formulation, which optimizes electricity generation to meet demand at minimized production cost. The objective function in (1) considers operating (c_k^t), startup ($c_k^{t,su}$), and shutdown ($c_k^{t,sd}$) costs associated with each generation unit (k) in each time period (t). Equation (2) represents the system load balance constraint where the sum of generation must equal the sum of load on all nodes (i) in each time period. Equations (3)–(5) model generator technical limitations. Equation (3) constrains committed generator outputs to within minimum (G^{MIN}) and maximum (G^{MAX}) output levels, (4) restricts the temporal shifts in generation to within ramping capabilities (M^{up}, M^{down}), and (5) connects the generator unit commitment status (u) with startup (su) and shutdown (sd) transitions. Energy production constraints are represented in (6), where generator energy output is constrained to a maximum ($E^{h,MAX}$) defined over some time period (h). Nodal power balance is defined in (7), where f represents the MW flow along each line (connecting nodes i and j). Kirchhoff's voltage law is represented by the linearized power flow formulation in (8), (9), where $B_{i,j}$ represents the susceptance of the transmission element connecting nodes i and j and θ represents bus voltage angles. Line flow limits are expressed by (10) and can represent thermal, stability, or other power transfer limits. Equation (11) specifies that unit commitment, startup, and shutdown variables must take on discrete (binary) values. The example formulation presented by (1)–(11) neglects the details required to appropriately represent storage devices [26], concentrating solar power facilities [27], and DC transmission infrastructure [28], and does
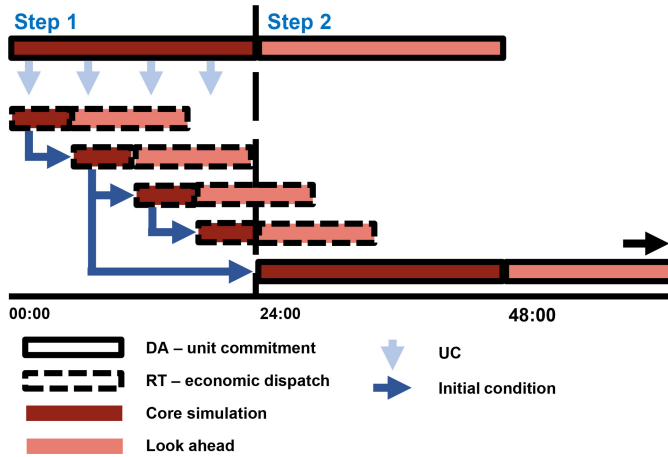
Fig. 5. Illustration of an example day-ahead and real-time market simulation.

TABLE V
RTS-GMLC DEFAULT SIMULATION PARAMETERS

Simulation Parameter	DAY-AHEAD	REAL-TIME
Periods/Step	24	1
Period Resolution	60 minutes	5 minutes
Date From	1/1/20	1/1/20
Date To	12/31/20	12/31/20
Look Ahead Periods/Step	24	2
Look Ahead Period Resolution	60 minutes	5 minutes
Reserve Products	$Flex_{Up}$, $Flex_{Dn}$, Reg_{Up}, Reg_{Dn}, $Spin_{Up}$	Reg_{Up}, Reg_{Dn}, $Spin_{Up}$

solution (core simulation) and discarding the remainder (look ahead). The RTS-GMLC includes default parameters for a day-ahead and real-time market simulation, which are summarized in Table V.

B. PCM Simulation Implementation

The RTS-GMLC can be analyzed using any standard commercial or open source PCM platform, and at the time of publication has been implemented in the PLEXOS [29], PSO [30], PowerWorld [31], Prescient [32], and Backbone [33] PCM software packages. We provide sample results from the Prescient, Backbone, and PLEXOS implementations below, each of which rely on expansions of the formulation of the problem posed in (1)–(11) above. PLEXOS is a commercially available and widely used energy systems optimization software developed by Energy Exemplar. Backbone is an open source model developed by VTT Technical Research Center of Finland and University College Dublin. Backbone can perform both investment and operational optimization with flexible time resolution and stochastic representation [34]. Backbone is written in GAMS and provides modeling flexibility to enable detailed modelling of specific systems as well large-scale system simulations. Besides electricity, new energy sectors, energy vectors, other processes, and material flows can be added through input data. Prescient is developed by Sandia National Laboratories specifically to allow for experimentation with advanced power grid operations models and strategies, and provides transparent implementations of those strategies. Prescient is an open source modeling package written in Python, with UC and ED optimization components written in the Pyomo open source optimization modeling language [35]. In addition to standard PCM simulation capabilities, Prescient includes state-of-the-art UC models, advanced methods for constructing probabilistic scenarios, and stochastic UC models and solvers.

Fig. 6 shows the hourly energy production results for a July week using Backbone, PLEXOS, and Prescient. The energy production results from each tool are summarizied by generation category over the sample July week in Table VI. The controlled experimental comparison excludes reserves, CSP generation, the DC transmission line, and the storage device, and demonstrates the suitability of the dataset for inclusion in a variety of PCM platforms. The PLEXOS and Backbone simulations are executed with identical parameters in a similar simulation framework, and the results are equivelent to within

not include representations of several modeling details, such as forced outages, generator up/down time constraints, fuel constraints, emissions constraints, and reserve/security constraints. This basic formulation can be amended to represent such devices and issues.

In addition to the core problem posed in (1)–(11), the example PCM formulation requires a chronological framework over which to optimize system operations. PCMs often consider a year-long simulation horizon in order to capture long-term intertemporal constraints and seasonal variability. A one-year simulation typically consists of 365 alternating day-ahead (UC) and real-time (ED) market optimizations (steps). Steps are solved in conjunction with a simulation engine which provides load, renewables, and contingency data. Fig. 5 applies the mathematical formulation in (1)–(11) to a simple day-ahead and real-time optimization cycle framework. The day-ahead simulation consists of a single UC optimization step that determines 24 hours of system operations subject to forecasted load and renewables. Subsequently the real-time simulation consists of 288 5-minute steps, which reoptimize the same 24 hours of system operations subject to actual load and renewables (redispatch). Because many baseload generators are inflexible at short timescales, the real-time simulation treats day-ahead baseload UC profiles as fixed constraints. However, peaking generators such as gas CTs may change commitment status in the real-time simulation.

A key challenge in implementing the example Fig. 5 framework is the preservation of inter-temporal constraints (e.g., ramp rates and minimum up and down times) between optimization steps via initial conditions. Here, each real-time step uses the previous real-time system state as its initial condition. Day-ahead steps mimic real-world market clearing practices by taking initial conditions from the previous day's midafternoon real-time solution (solved forward to midnight using adjusted forecast data). A further challenge is that ignorance of future conditions can cause suboptimal decision-making at the ends of optimization steps. The example framework avoids so-called end-of-horizon effects by requiring the day-ahead and real-time simulations to solve 48 hours and 15 minutes respectively at a time, keeping only the first 24 hours and 5 minutes of each
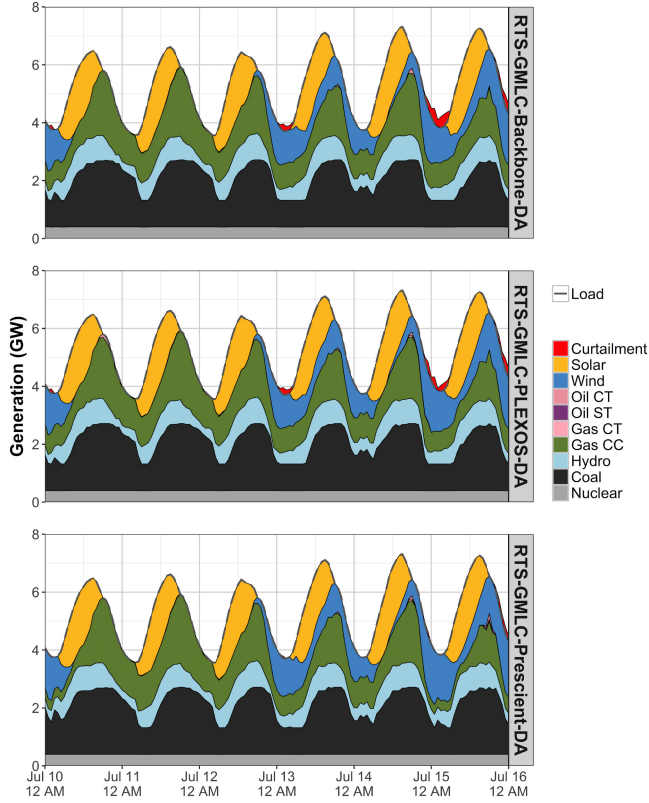
Fig. 6. Hourly energy production from a day-ahead market simulation for a July week using Backbone (top), PLEXOS (middle), and Prescient (bottom).

TABLE VI
RTS-GMLC ENERGY PRODUCTION (MWH) RESULTS BY GENERATION
CATEGORY FOR A JULY 10–15 DAY-AHEAD SIMULATION

Category	Backbone	PLEXOS	Prescient
Curtailment	4.72	3.80	1.32
Solar	110.60	111.58	110.86
Wind	80.71	80.93	84.82
Oil CT	0.38	0.23	0.60
Oil ST	0.00	0.00	0.00
Gas CT	0.00	0.89	0.36
Gas CC	176.69	174.40	163.47
Hydro	94.00	94.00	94.00
Coal	245.89	246.24	254.12
Nuclear	57.88	57.89	57.94
Total	766.16	766.16	766.16

the 0.1% optimality tolerances. Prescient is designed to more explicitly reflect market clearing processes and executes with representations of the day-ahead market clearing and realized system operations in a nested framework. While the example results are simulated without any forecast error, the discrepancies in simulation framework generate slightly different results since the model includes a real-time re-optimization subject to a shorter optimization horizon (4 hr) that facilitates commitment and dispatch deviations after the day-ahead market clearing. Furthermore, because the optimization problem formulation and simulation process used by PLEXOS is proprietary, it is impossible to exactly diagnose the exact differences between the
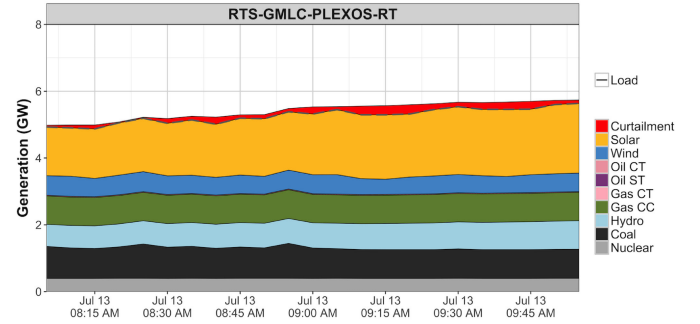

Fig. 7. Five-minute energy production from a real-time market simulation for a two hour period on July 13 using PLEXOS.
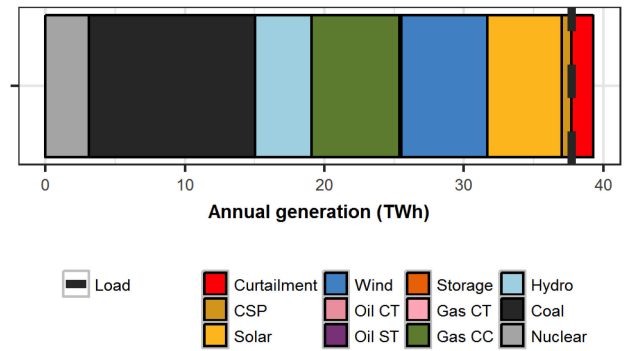

Fig. 8. Sample annual energy production from a day-ahead market simulation using PLEXOS.

PLEXOS and the other tools. Fig. 7 shows energy production results at 5-minute resolution from a real-time market simulation using PLEXOS. Finally, Fig. 8 shows annual energy by resource for a year-long PLEXOS day-ahead simulation. Notably, the RTS-GMLC optimization results (PLEXOS) exhibit congestion (one or more binding transmission flow limits) 18.6% of the year (1,632 hours), whereas optimal PCM solutions of the published RTS-96 data are never congested. In addition, the optimal scheduling of the RTS-GMLC fleet results in an annual renewable (Wind, Solar, Hydro) energy penetration of 25.1%, with 22.2% of the available wind and solar energy curtailed.

C. System Reliability Indices

Reference reliability indices for the system are provided based on two nonsequential assessment methods. First, classical capacity outage probability table analysis [36] was performed for each time period to generate hourly loss-of-load probability (LOLP) and expected unserved energy (EUE) values. Second, Monte Carlo sampling [37] with a "pipe-and-bubble" transport model was applied with 100,000 samples in each timestep to capture the possible composite reliability impacts of transfer limits and outage probabilities on interregional lines. For both approaches, annual aggregate statistics are reported in Table VII and full

TABLE VII
RTS-GMLC Reference Annual Reliability Statistics

Metric	COPT	Monte Carlo (three-region): estimate $\pm$ standard error
LOLE[3] (h/year)	0.00189808	0.0017 ± 0.0001
EUE (MWh/year)	0.233809	0.24 ± 0.03
NEUE (ppm)	0.00620911	0.0064 ± 0.0008

hourly results are included in the RTS-GMLC GitHub repository [22].[3]

The composite reliability results obtained from Monte Carlo sampling are statistically indistinguishable from the exact generation reliability results from the capacity outage probability table (COPT), indicating that interregional transmission considerations contribute very little, if at all, to shortfall risk. In both cases the reliability metrics are very low, indicating that the addition of variable generation to the RTS-96 without reducing the aggregate capacity of conventional generation results in a system that is significantly overbuilt. This allows for adjusting the availability of certain generation resources to study different development patterns as desired while maintaining acceptable reliability levels.

The RTS-86 paper gives "exact" reliability indices for a two area version of the RTS-79 system [3]. Preston and Barrows adopt the methods used to generate the RTS-86 paper indices and calculate the "exact" reliability indices for the RTS-GMLC in [38] for two example load levels. While the RTS-86 paper used a full binary tree to evaluate all the generator outage probability states without rounding assumptions for every hour in a test year, the programmatic implementation in [38], RTS3, develops an "exact" COPT, also without rounding assumptions, to find the hourly LOLPs for the 2020 test year. The COPT is not size-limited; however, the generators must be independent and integer-valued to give "exact" LOLPs for the non-integer load served every hour. Since wind and solar are weather dependent, they are treated as load reducers in the RTS3 study files. The RTS3 data, program and output reports are available on GitHub (see Section III-C) for others to benchmark their models against.

V. Conclusion

We implemented a variety of updates to the RTS generation and load, resulting in the RTS-GMLC. This new test system includes modern generating resources with unique heat rate assignments derived from real-world data, and a geographically coherent 5-minute time series dataset for wind, solar, and load. The update also includes power forecasts for load, wind, utility-scale PV, rooftop PV and CSP resources at hourly resolution. The resulting RTS-GMLC dataset presents unique opportunities to examine issues related to reliabile operation and planning of power systems while considering the availabilty of forecasted and actual time series for wind and solar generation and real power demand. The example applications presented

in Section IV demonstrate the dataset usability, and show that the RTS-GMLC system has excess generation capacity. Thus, the RTS-GMLC provides users with numerous options to include subsets of the generation fleet to examine alternate fleet configurations, to explore opportunities to increase renewable usage, or to explore a variety of other issues through system modification or augmentation. While the majority of the RTS-GMLC updates have been made to improve quality and applicability of the dataset to modern power systems operations and planning studies, we have preserved the extent of the RTS-96 dataset in order to enable studies of system reliability and stability.

The updated model is published on GitHub to facilitate dissemination and encourage collaboration. Individuals interested in using the RTS-GMLC to explore modern power systems are encouraged to collaborate and contribute modifications. As the evolution of the RTS continues, future versions of the test system will be tagged and released through technical publications. In addition to the updated data presented here, the repository includes formatted datasets for several common modeling tools, including: PLEXOS, MATPOWER, PSO, PowerWorld, PSS/E, Prescient, and Backbone [24], [25], [29]–[33]. Every attempt has been made to create a dataset that reflects many of the challenges posed by modern power systems, however the effort is certainly incomplete. Obvious candidates for future data augmentation include: capacity cost and resource availability information, different variable generation mixes, improved generator dynamic models, improved representations of storage resources, and time and price responsive demand information.

---

[3] When calculated over all hours of a year (as is done here), LOLE is sometimes also referred to as LOLH (loss-of-load hours) to distinguish it from calculations considering only peak daily net load hours.

Laboratory. Sandia National Laboratories is a multimission laboratory managed and operated by National Technology and Engineering Solutions of Sandia, LLC, a wholly owned subsidiary of Honeywell International, Inc., for the U.S. Department of Energy's National Nuclear Security Administration under Contract DE-NA-0003525. This paper describes objective technical results and analysis. Any subjective views or opinions that might be expressed in the paper do not necessarily represent the views of the U.S. Department of Energy or the United States Government.

REFERENCES

[1] C. Coffrin, D. Gordon, and P. Scott, "NESTA, The NICTA Energy System Test Case Archive," Nov. 2014, *arXiv:1411.0359*. [Online]. Available: http://arxiv.org/abs/1411.0359

[2] P. M. Subcommittee, "IEEE Reliability Test System," *IEEE Trans. Power App. Syst.*, vol. PAS-98, no. 6, pp. 2047–2054, Nov. 1979.

[3] R. N. Allan, R. Billinton, and N. M. K. Abdel-Gawad, "The IEEE reliability test system—Extensions to and evaluation of the generating system," *IEEE Trans. Power Syst.*, vol. 1, no. 4, pp. 1–7, Nov. 1986.

[4] C. Grigg *et al.*, "The IEEE Reliability Test System-1996. A report prepared by the reliability test system task force of the application of probability methods subcommittee," *IEEE Trans. Power Syst.*, vol. 14, no. 3, pp. 1010–1020, Aug. 1999.

[5] "Power Systems Test Case Archive—UWEE," Dec. 2018. [Online]. Available: http://labs.ece.uw.edu/pstca/

[6] C. Josz, S. Fliscounakis, J. Maeght, and P. Panciatici, "AC power flow data in MATPOWER and QCQP format: iTesla, RTE Snapshots, and PEGASE," Mar. 2016, arXiv:1603.01533.

[7] K. W. Hedman, R. P. O'Neill, E. B. Fisher, and S. S. Oren, "Optimal transmission switching with contingency analysis," *IEEE Trans. Power Syst.*, vol. 24, no. 3, pp. 1577–1586, Aug. 2009.

[8] J. McCalley *et al.*, "Probabilistic security assessment for power system operations," in *Proc. IEEE Power Eng. Soc. Gen. Meeting*, Jun. 2004, pp. 212–220.

[9] A. L. Motto, F. D. Galiana, A. J. Conejo, and J. M. Arroyo, "Network-constrained multiperiod auction for a pool-based electricity market," *IEEE Trans. Power Syst.*, vol. 17, no. 3, pp. 646–653, Aug. 2002.

[10] D. Lew *et al.*, "The western wind and solar integration study phase 2," Nat. Renew. Energy Lab., Golden, CO, USA, Tech. Rep. NREL/TP-5500-55588, Sep. 2013. [Online]. Available: https://www.nrel.gov/docs/fy13osti/55588.pdf

[11] Western Electricity Coordinating Council (WECC), "TEPPC 2011 Study Program 10-Year Regional Transmission Plan," Western Electricity Coordinating Council Transmission Expansion Planning Policy Committee, Salt Lake City, UT, Tech. Rep., 2011. [Online]. Available: www.wecc.org/Reliability/2011Plan_2020%20Study%20Report.pdf

[12] P. Gilman, "SAM Photovoltaic Model Technical Reference," Nat. Renew. Energy Lab., Golden, CO, USA, Tech. Rep. NREL/TP-6A20-64102, May 2015. [Online]. Available: https://www.nrel.gov/docs/fy15osti/64102.pdf

[13] J. Jorgenson, P. Denholm, M. Mehos, and C. Turchi, "Estimating the performance and economic value of multiple concentrating solar power technologies in a production cost model," Nat. Renew. Energy Lab., Golden, CO, USA, Tech. Rep. NREL/TP-6A20-58645, Dec. 2013. [Online]. Available: https://www.nrel.gov/docs/fy14osti/58645.pdf

[14] J. Jorgenson, M. O'Connell, P. Denholm, J. Martinek, and M. Mehos, "A guide to implementing concentrating solar power in production cost models," Nat. Renew. Energy Lab., Golden, CO, USA, Tech. Rep. NREL/TP-6A20-68527, 2018.

[15] P. Denholm, J. Jorgenson, M. Hummon, T. Jenkin, and D. Palchak, "The value of energy storage for grid applications," Nat. Renew. Energy Lab., Golden, CO, USA, Tech. Rep. NREL/TP-6A20-58465, May 2013. [Online]. Available: https://www.nrel.gov/docs/fy13osti/58465.pdf

[16] C. Ruchti, H. Olia, K. Franitza, and A. Ehrsam, "Combined cycle power plants as ideal solution to balance grid fluctuations—Fast start-up capabilities," in *Proc. 43th Colloq. Power Plant Technol.*, Jan. 2011, pp. 18–19.

[17] L. Balling, "Flexible future for combined cycle," pp. 61–65, 2010.

[18] J. Niemi, "Combustion Engine vs Gas Turbine—Startup time," 2017. [Online]. Available: https://www.wartsila.com/energy/learning-center/technical-comparisons/combustion-engine-vs-gas-turbine-startup-time

[19] "KA26 Fast Start Gas Turbine Upgrade | GE Power," 2017. [Online]. Available: https://powergen.gepower.com/services/upgrade-and-life-extension/gas-turbine-upgrades/gas-turbine-upgrades-catalog/ka26-fast-start.html

[20] M. Rossol *et al.*, "An analysis of thermal plant flexibility using a national generator performance database," *Environ. Sci. Technol.*, submitted for publication.

[21] E. Ibanez, G. Brinkman, M. Hummon, and D. Lew, "Solar reserve methodology for renewable energy integration studies based on sub-hourly variability analysis," in *Proc. 2nd Annu. Int. Workshop Integr. Sol. Power Power Syst. Conf.*, Nov. 2012. [Online]. Available: https://www.nrel.gov/docs/fy12osti/56169.pdf

[22] "RTS-GMLC: Reliability Test System—Grid Modernization Lab Consortium," Apr. 2018. [Online]. Available: https://github.com/GridMod/RTS-GMLC

[23] G. B. Sheble and G. N. Fahd, "Unit commitment literature synopsis," *IEEE Trans. Power Syst.*, vol. 9, no. 1, pp. 128–135, Feb. 1994.

[24] M. Prötzsch, "PSSE—High-performance transmission planning and analysis software," Apr. 2018. [Online]. Available: https://www.siemens.com/global/en/home/products/energy/services/transmission-distribution-smart-grid/consulting-and-planning/pss-software/pss-e.html

[25] R. D. Zimmerman, C. E. Murillo-Sanchez, and R. J. Thomas, "MAT-POWER: Steady-state operations, planning, and analysis tools for power systems research and education," *IEEE Trans. Power Syst.*, vol. 26, no. 1, pp. 12–19, Feb. 2011.

[26] C. A. Silva-Monroy and J. Watson, "Integrating energy storage devices into market management systems," *Proc. IEEE*, vol. 102, no. 7, pp. 1084–1093, Jul. 2014.

[27] M. Hummon, P. Denholm, J. Jorgenson, and M. Mehos, "Modelling concentrating solar power with thermal energy storage for integration studies," Preprint, p. 10, 2013.

[28] Y. V. Makarov *et al.*, "Models and methods for assessing the value of HVDC and MVDC technologies in modern power grids," Pacific Northwest Nat. Lab., Richland, WA, USA, Tech. Rep. PNNL-26640, 2017.

[29] "Energy Exemplar »Energy Market Modelling," May 2016. [Online]. Available: http://energyexemplar.com/

[30] "Polaris—Power Systems Optimization," Apr. 2018. [Online]. Available: http://psopt.com/

[31] "PowerWorld »The visual approach to electric power systems," Apr. 2018. [Online]. Available: https://www.powerworld.com/

[32] B. Knueven, J. Ostrowski, and J. P. Watson, "A novel matching formulation for startup costs in unit commitment," *Optim. Online*, Mar. 2017.

[33] N. Helistö *et al.*, "Backbone—An adaptable energy systems modelling framework," submitted for publication. [Online]. Available: cris.vtt.fi/en/publications/backbone-an-adaptable-energy-systems-modelling-framework

[34] J. Miettinen, J. Ikäheimo, T. Rasku, H. Holttinen, and J. Kiviluoma, "Impact of longer stochastic forecast horizon on the operational cost of a power system," in *Proc. 15th Int. Conf. Eur. Energy Market*, Lodz, Poland, Jun. 2018, pp. 1–5.

[35] W. E. Hart, C. Laird, J.-P. Watson, and D. L. Woodruff, *Pyomo—Optimization Modeling in Python*, vol. 67, 2nd ed. New York, NY, USA: Springer, 2017.

[36] R. Billinton, *Power System Reliability Evaluation*. New York, NY, USA: Taylor & Francis, 1970.

[37] R. Billinton and W. Li, *Reliability Assessment of Electric Power Systems Using Monte Carlo Methods*. New York, NY, USA: Springer, 1994. [Online]. Available: //www.springer.com/us/book/9780306447815

[38] E. Preston and C. Barrows, "Evaluation of year 2020 IEEE RTS generation reliability indices," in *Proc. IEEE Int. Conf. Probab. Methods Appl. Power Syst.*, Jun. 2018, pp. 1–5.